arXiv:2305.14730v2 [cs.CV] 30 Aug 2023

BinaryViT: Towards Efficient and Accurate Binary Vision Transformers

Junrui Xiao[1,2], Zhikai Li[1,2], Lianwei Yang[1,2], Qingyi Gu[1]*
[1]Institute of Automation, Chinese Academy of Sciences. Beijing, China
[2]School of Artificial Intelligence, University of Chinese Academy of Sciences. Beijing, China
{xiaojunrui2020, lizhikai2020, yanglianwei2021, qingyi.gu}@ia.ac.cn

Abstract

Vision Transformers (ViTs) have emerged as the fundamental architecture for most computer vision fields, but the considerable memory and computation costs hinders their application on resource-limited devices. As one of the most powerful compression methods, binarization reduces the computation of the neural network by quantizing the weights and activation values as ± 1. Although existing binarization methods have demonstrated excellent performance on Convolutional Neural Networks (CNNs), the full binarization of ViTs is still under-studied and suffering a significant performance drop. In this paper, we first argue empirically that the severe performance degradation is mainly caused by the weight oscillation in the binarization training and the information distortion in the activation of ViTs. Based on these analyses, we propose **BinaryViT**, an accurate full binarization scheme for ViTs, which pushes the quantization of ViTs to the limit. Specifically, we propose a novel gradient regularization scheme (GRS) for driving a bimodal distribution of the weights to reduce oscillation in binarization training. Moreover, we design an activation shift module (ASM) to adaptively tune the activation distribution to reduce the information distortion caused by binarization. Extensive experiments on ImageNet dataset show that our BinaryViT consistently surpasses the strong baseline by 2.05% and improve the accuracy of fully binarized ViTs to a usable level. Furthermore, our method achieves impressive savings of 16.2$\times$ and 17.7$\times$ in model size and OPs compared to the full-precision DeiT-S.

1 Introduction

Transformer-based model recently emerges as a common but effective architecture and have achieved remarkable performance improvement in various computer vision fields, such as image classification [7, 10, 14, 40], object detection [6, 41, 42] and semantic segmentation [37, 50]. However, the huge energy, computation, and memory costs of vision transformers (ViTs) make their deployment on resource-limited devices still challenging, which hinders the practical applications of ViTs in real-world. Therefore, there is an urgent need to compress ViTs and improve their inference efficiency for real-world applications.

Various model compression methods have been proposed to alleviate resource constraint issue and speed up inference, such as pruning [13, 48], knowledge distillation [18, 34, 45], quantization [15, 17, 24, 43], and dynamic token reduction [3, 32, 46]. Among those methods, quantization is an effective and general compression technique that converts network weights and activation from 32-bit floating-point values to low-bit fixed-point representations. Previous efforts [15, 19, 24] aimed to quantize pre-trained ViTs to the lowest possible bit-width with only a minor performance degradation. As the extreme limit of quantization, binarization compacts the weight and activation to ± 1, which can eliminate multiplication operations altogether and employ bit-wise XNOR operations [5] instead.

Preprint. Under review.

Theoretically, binarization can promise up to 32× reduction in model size and achieve energy efficiency gains of 100-1000× compared to full-precision models [28].

The main challenge of binarization lies in the fact that an extremely low bit-width (*e.g.*, 1-bit) lead to information distortion, making it difficult to optimize. On the one hand, most of the previous binarization methods [5, 23, 25] in computer vision are designed for convolutional neural networks (CNNs), such as RPReLU [23] and extra skip connections [33], which have not generalized well to transformer models. On the other hand, there are also many efforts [1, 22, 30] to binarize transformer architectures in natural language processing tasks, such as bi-attention [30] and elastic binarization [22], but the larger and more complex features of ViTs pose new challenges for its binarization. As a result, existing methods cannot be extended and migrated well due to significant differences in model architecture and tasks, leaving binarization for ViTs as a gap.

To enhance the accuracy of binary ViTs, we first build a fully binary ViT baseline, a straightforward yet effective solution based on common techniques. We empirically analyze the strong baseline and find the performance degradation lies on the weight oscillation and the information distortion in the activation. As shown in Figure 1, we find that the straight-through estimator (STE) [2] in optimizer induces a bell-shaped distribution of weights (or even a delta distribution), which causes most of the weights near zero to be randomly binarized, resulting in unstable weights in training. Then by further studying the internal variation of activation, we discover that drastic inter-channel and inter-token variation makes the binarization for activation sub-optimal, as in Figure 2, leading to more information distortion.

Motivated by the analysis above, we propose an accurate full binarization scheme for ViTs, namely BinaryViT, to push the limit of 1-bit ViT models. To tackle the oscillation in training, we introduce a gradient regularization scheme (GRS) to build an adaptive optimization objective. GSR induces the weights into a bimodal distribution, thus reducing the stochasticity of the weights in the binarization. Moreover, we develop an activation shift module (ASM) to compensate the distribution of activation in uniform binarization. Extensive experiments on the ImageNet dataset [35] have shown that our BinaryViT performs very well across various transformer architectures, such as DeiT [39], ViT [10], and consistently surpasses strong baselines. In general, our contributions are listed as follows:

- We propose a gradient regularization scheme (GRS) to address the weight oscillation issue in binarization training. GRS induces a bimodal distribution of weights, and thus makes them discriminatory to eliminate binarization stochasticity.
- To mitigate drastic internal variation, we develop an activation shift module (ASM) that can tune distribution of activation by using a learnable shift factor, allowing the binarized model to recover the representation of the input image as much as possible.
- Extensive experiments conducted on various ViTs architecture demonstrate the effectiveness of our proposed method. The results show that our BinaryViT consistently outperforms current baselines by great margins and achieves comparable performances.

2 Related Works

Efficient Vision Transformers. Inspired by the success in natural language processing, transformer-based architectures have been widely adopted and significantly improved accuracy on various computer vision tasks. For instance, ViT [10] splits images into a sequence of flattened tokens (*i.e.*, patches) as input tokens, with each block featuring a multi-head self-attention (MHSA) mechanism that extracts capturing long-distance visual relations. Subsequently, DeiT [39] and Swin Transformer [21] make several improvements to ViT, enhancing its efficiency and generalization capability. Despite demonstrating great potential across various tasks, the large memory, computation, and energy consumption of ViTs hinder their deployment on resource-limited devices, such as mobile devices and wearables. Several works have attempted to alleviate resource constraint issue and take trade-off between performance and efficiency. MobileViT [26] attempts to incorporate transformer into MobileNetV2 [36] and proposes a hybrid block to enhance the local-global representation and spatial order preservation. Performers, Flashattention [9] and Hydra attention [4] attempts to design faster attention to speed up inference. Adavit [27] and Dynamic ViT [32] introduces model pruning to remove redundant heads and features, achieving competitive efficiency and performance trade-offs. ToMe [3] propose dynamic token combination mechanisms that gradually merge tokens in inference to increase efficiency. FQ-ViT [19] quantizes LayerNorm and Softmax operations to obtain fully

quantized ViTs. Q-ViT [15] introduces distillation to improve the performance of quantized ViTs. While plenty of works [16, 17, 24, 49] also have proposed quantization schemes for ViTs, very few have focused on binarization.

Binarization. Considering the immense potential of reducing memory and practical computational costs, binary neural networks (BNNs) have been widely studied in the recent years. Binarization began with Binaryconnect [8], which propose a back-propagation scheme for training the discrete binary weights. After that, XnorNet [33] employed a float point scaling factor for each weight kernels and use xor and popcnt replace multiple operations, which makes significant improvement on the accuracy of BNNs. Real-to-binary [25] and ReActNet [23] attempts to design a binary-friendly architecture and built a strong baseline upon CNNs. IR-Net [31] propose a soft sign function for SGD optimizer to better model continuous gradient propagation. The proposed methods achieved competitive performance on traditional CNNs but cannot generalize well to transformer models. As for binary transformers, there are several works proposed in NLP tasks. BinaryBert [1] have pushed down the weight and word embedding to be binarized, but its activation still keeps on 8/4 bit. BiBert [30] develop a fully binarization scheme with well-designed attention and distillation. Inspired by ReActNet, BiT [22] designed an elastic binary function and used progressive distillation to further improve accuracy of binary Bert. However, the larger and more complex features pose new challenges for its binarization, e.g., the dense feature refinement methods used in NLP do not work for ViTs.

These excellent methods have inspired current research. In this paper, we make a further step to explore the efficient and accurate binarization scheme for effective inference of ViTs.

3 Building a strong binary ViTs baseline

In this section, we first build a vanilla binarized ViT model, since it has never been proposed in previous works. And then, we bring together some best practices in binary CNNs that can help us build a strong baseline of binary ViTs.

3.1 Binarized ViTs

In standard ViTs, the input data first passes through an embedding layer before being fed into the transformer blocks. Each transformer block consists of a MSA module and a MLP. Denoting the input features to MSA in the l^{th} layer by $X^l \in \mathbb{R}^{N\times d}$, where N is the sequence length and d is the embedding dimension, the MSA and MLP can be formulated as:

$$\text{MSA}(X^l) = \text{Concat}[\text{softmax}(\frac{Q_h^l {K_h^l}^T}{\sqrt{d_h}})V_h^l W_o^l]_{h=1}^H, \quad \text{MLP}(Z^l) = \sigma(Z^l W_1^l + b_1^l)W_2^l + b_2^l, \quad (1)$$

where $Z^l = \text{LN}(\text{MSA}(X^l) + X^l)$ represents the input of MLP, σ denotes the nonlinear activation function (*e.g.*, GELU), and $W_1, W_2^T \in \mathbb{R}^{d\times d'}$, $b_1 \in \mathbb{R}^{d'}$, $b_2 \in \mathbb{R}^d$ are projection matrices and biases, respectively. h is the number of attention head.

In a tranformer block, we denote its weight set as $\mathbf{W} = \{\mathbf{w}^l\}_{l=1}^L$ and input activations as $\mathbf{A} = \{\mathbf{a}_{in}^l\}_{l=1}^L$. Thus, the computation can be expressed as:

$$\mathbf{a}_{out}^l = \mathbf{w}^l \otimes \mathbf{a}_{in}^l \quad (2)$$

where $\otimes$ denotes the matrix multiplication in fully connected layer. As for binarization, we quantize the weights and activations to 1-bit representation by applying $\text{Sign}(x)$ in forward propagation. And then, the float point multiplication can be approximated by the efficient XNOR and Bit-count operators, which can be expressed as:

$$\mathbf{a}_{out}^l = \alpha^l \circ (\text{Sign}(\mathbf{w}^l) \odot \text{Sign}(\mathbf{a}_{in}^l)) \quad (3)$$

where $\circ$ and $\odot$ presents channel-wise multiplication and efficient bit-wise operations, respectively. $\alpha_{\mathbf{w}}^l$ is the channel-wise scaling factors for weight to minimize the quantization error. Most existing implementations simply follow XnorNet [33] to compute $\alpha_{\mathbf{w}}^l$ as $\frac{\|\mathbf{w}^l\|_{l1}}{n}$. We apply the STE [2] to calculate the non-derivable gradients in backward propagation, which can be formulated as:

$$\frac{\partial \mathcal{L}}{\partial x} = \frac{\partial \mathcal{L}}{\partial \,\text{Sign}(x)} \frac{\partial \,\text{Sign}(x)}{\partial x} = \begin{cases} \frac{\partial \mathcal{L}}{\partial \,\text{Sign}(x)} & \text{if } x \in [-1, 1]\,, \\ 0 & \text{otherwise} \end{cases} \quad (4)$$

3.2 Training techniques

Learnable scaling factors. The non-parametric factor is simple but cannot guarantees on optimizing network performance. Inspired by LSQ [11], we seek to minimize task loss by using a learnable layer-wise scaling factor. By reformulating $\hat{x} = \mathrm{Sign}(x)$ to $\hat{x} = \lfloor \mathrm{Clip}\left(x, -1, 1\right) \rceil$, we introduce a learnable scaling factor $\alpha^l \in \mathbb{R}$ to approximate the gradients precisely, which can be expressed as:

$$\mathbf{x}^l \approx \alpha^l \hat{\mathbf{x}}^l = \alpha^l \cdot \left\lfloor \mathrm{Clip}\left(\frac{\mathbf{x}^l}{\alpha^l}, -1, 1\right) \right\rceil \tag{5}$$

where the $\lfloor \cdot \rceil$ is the round function. In addition, the binarized values $\hat{\mathbf{x}}^l$ are used in inference, and the full-precision weight $\mathbf{x}^l$ only serve as proxies for computing gradints and are commonly referred to as latent weights. Following the common practice in [5, 23, 33], we use STE to computer the gradients of α^l in backward propagation:

$$\frac{\partial \hat{\mathbf{x}}^l}{\partial \alpha^l} = \begin{cases} -1 & \frac{\mathbf{x}^l}{\alpha^l} <= -1 \\ -\frac{\mathbf{x}^l}{\alpha^l} + \lfloor \frac{\mathbf{x}^l}{\alpha^l} \rceil & -1 < \frac{\mathbf{x}^l}{\alpha^l} < 1 \\ 1 & \frac{\mathbf{x}^l}{\alpha^l} >= 1 \end{cases} \tag{6}$$

Consequently, we train α^l with gradients from the final task loss.

Two-step binarization. Due to the large gap between the full precision model and the binary model, the direct binarization for full precision model will lead to severe degradation of performance. Inspired by Real-to-Binary [25] and ReActNet [23], we mitigate the gap by applying the two-stage training scheme.

Simple knowledge distillation. Previous BERT model binarization works [1, 22, 30] attempt to distill the attention scores and dense features. However, we provide experiments to show that feature distillation are not suitable for ViTs. In this work, we just use the logits distillation to enhance the performance of the baseline. And the final task loss can be formulated as:

$$\mathcal{L}_{total} = (1 - \lambda_d) \cdot \mathcal{L}_{pred} + \lambda_d \cdot \mathcal{L}_{distill} \tag{7}$$

By combining these techniques, we are able to establish a strong baseline that improves Top-1 Accuracy by 4.1% compared to vanilla binarized DeiT-Tiny (Results are shown in Section 5.2).

4 Approach

In this section, We first investigate the performance upper bound of the strong baseline, identify its main performance hindrance in Section 4.1. Then in Section 4.2 and Section 4.3, we propose two novel Binarization methods, gradient regularization scheme (GRS) and activation shift module (ASM), for weight and activation respectively.

4.1 Motivation

Empirically, the performance of standard binary ViTs is observed to undergo a significant decline, attributable to the weight oscillation and distortion introduced by quantizers, which diminish the model's representational capability. To investigate the issues mentioned above, we have visualized the weights and activation values and analyzed them as follows.

Oscillation in weight. As the simple but useful technique, STE and learnable scaling factors are widely adopted in existing quantization methods. Following the rule of STE, the gradient of weight can be computed as Eq. (10) that means the gradient of the binary weight as same as the latent weight within the quantization boundary. However, the latent weights oscillating around the center of quantization bin causes implicit stochasticity during the binary training. As shown in Figure 1, we observe that the learned latent weights tend to cluster around their mean centers, and the distribution exhibits a pronounced peak near 0, which coincides with previous observations [20, 44]. We argue that the closer the latent weights are to the point 0 (*i.e.*, the center of the quantized bin), the more easily their gradients are reversed, leading to the weights oscillation[1] Thus, it requires a regularization scheme to induce a bimodal distribution of weights that can solve the oscillation problem.

[1] .

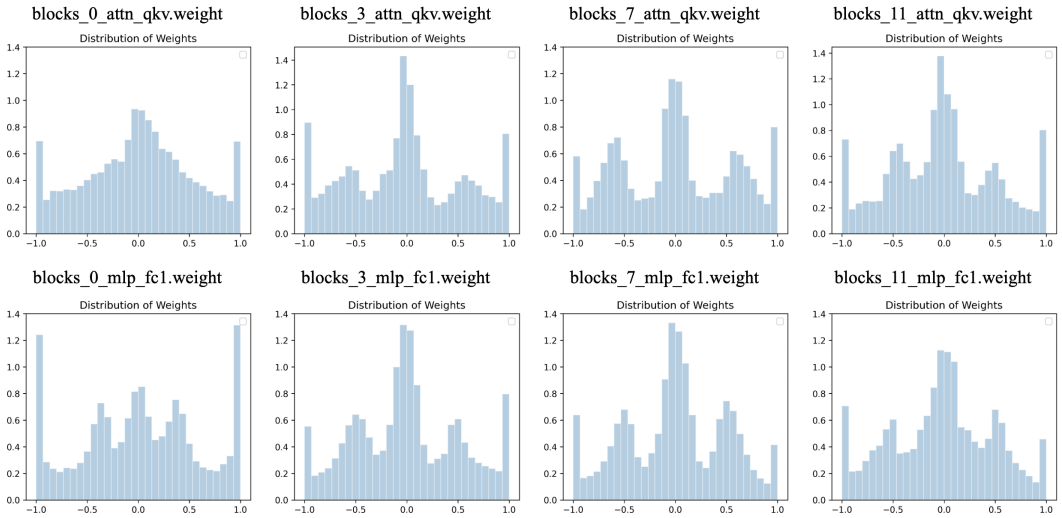

Figure 1: The histogram of latent weight distribution. We visualize the distribution of latent weights and found that a significant number of weights are heavily concentrated around 0, which increases the stochasticity of binarization and the possibility of gradient inversion.

Distortion in activation. As discussed in [17, 19, 49], quantized activations exhibit significant inter-channel variation, which poses a critical limitation to quantization performance. We further observe that these drastic variations in binary ViT activations exist not only channel-wise but also among tokens. As illustrated in Figure 2, we plot the distribution boxplot for the 175th to 225th channels of the activation from the last MLP layer in ViT-S[10]. Applying a uniform threshold to each channel or token fails to accommodate such severe inter-channel variation, resulting in substantial information distortion. Alternatively, channel-wise quantization can address this issue, but it requires dedicated hardware. We argue that adaptively tuning the activation distribution before the quantization process can tackle the aforementioned challenge. Therefore, designing an activation shift module is crucial for mitigating the distortion problem.

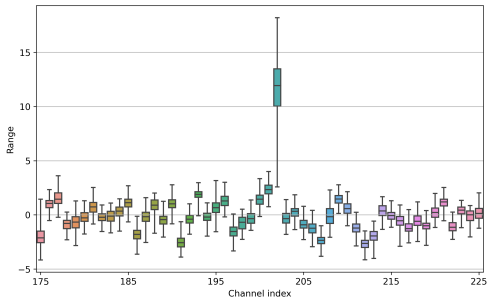

Figure 2: The box represents the quartiles of the values, and the whiskers extend to show the maximum and minimum values. The results indicate that there are significant variations in the channel-wise distribution and uniform binarization may lead to more severe information degradation.

4.2 Gradient regularization

As mentioned above, applying STE to compute the gradient of discrete weights can cause weights smaller than the scaling factors to gradually shrink toward center of the quantization bin and eventually oscillate around the threshold, *i.e.*, 0. To prevent this issue and avoid driving weights to 0 during binary training, we need to induce a bimodal distribution of weights centered at ± 1. Mean absolute error (MAE) and mean square error (MSE) can be used to drive the weights to ± 1. Following this intuition, we can define the function as:

$$\mathcal{L}_1 = \sum_{l=0}^{L} |\alpha^l - |\mathbf{w}^l||, \quad \mathcal{L}_2 = \sum_{l=0}^{L} (\alpha^l - |\mathbf{w}^l|)^2 \tag{8}$$

where the α^l is the leanable scaling factors as defined in Eq. (5). Note that, since the scale factors are applied to relax the hard binary values ± 1, the weights should be induced to shrink to the vicinity of the scale factors α^l. This leads to a symmetric regularization function with two minimums, one at $-\alpha^l$ and another at $+\alpha^l$ (as shown in Figure 3). However, the gradient of each transition point is

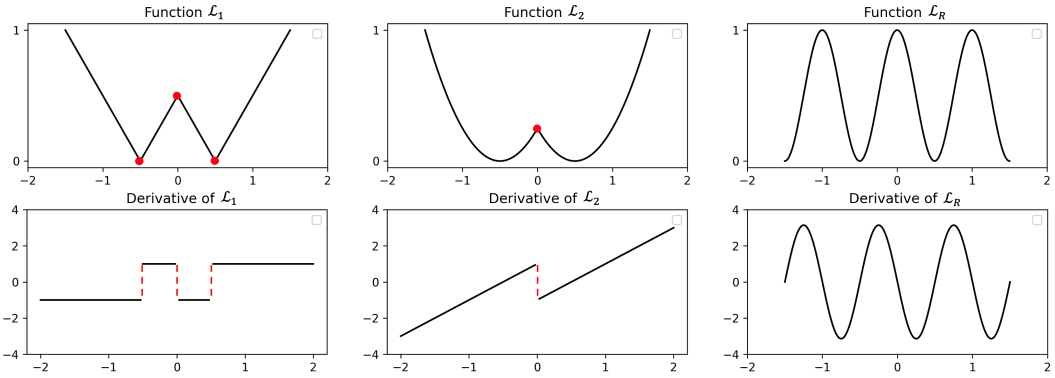

Figure 3: The comparison of $\mathcal{L}_1$, $\mathcal{L}_2$, and $\mathcal{L}_R$.As a toy example, the **red** dot represents the transition point, and α^l is set to 0.5. Unfortunately, the gradients of $\mathcal{L}_1$ and $\mathcal{L}_2$ are undefined at the transition point, causing the direction of the update to reverse and resulting in an unstable training process. In contrast, the proposed $\mathcal{L}_R$ is smooth everywhere and its magnitude does not decrease with α^l, but rather remains at a stable value.

undefined in MAE and MSE, which will hinder the propagation of the gradient in each layer. What's worse, the magnitude of their penalty is positively related to α^l. That means that smaller weights near 0 are hardly penalized. To alleviate the gradient issue, we propose a gradient regularization scheme (GRS) that smooth everywhere and will significantly reduce the weight oscillation. We define the continuous and differentiable regularization term as follows:

$$\mathcal{L}_R = \sum_{l=0}^{L} \cos^2(\pi * \frac{\mathbf{w}^l}{2\alpha^l}) \tag{9}$$

where α^l is the scaling factors and controls the shrink center of latent weight. Based on GRS, we now give the gradients of $\mathcal{L}_R$ as:

$$\frac{\partial \mathcal{L}_R}{\partial \mathbf{w}} = -\frac{\pi}{\alpha} \sum_{l=0}^{L} \sin(\pi * \frac{\mathbf{w}^l}{\alpha^l}) \cos(\pi * \frac{\mathbf{w}^l}{\alpha^l}) \tag{10}$$

As illustrated in Figure 3, our GRS is smooth everywhere and drives the latent weight to the $\pm\alpha^l$, which can reduce the gradient reverse issue. Note that, to prevent any negative interactions with the quantization scale gradient, we follow [11] to clip our latent weights to the range of the quantization bin, allowing only unclipped weights to receive regularization.

4.3 Activation shift

To tackle the issue of distortion in activation caused by severe internal variation, we propose an activation shift module (ASM) that leverages the original features to learn an adaptive shift factor, which tuning the distribution of activation adaptively and can better preserve the semantic information in sign function.

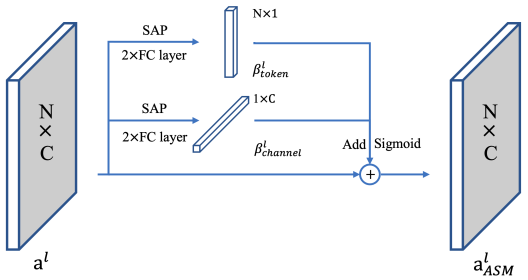

Figure 4: The ASM in BinaryViT, which employs a dynamic redistribution scheme for the latent activation.

As shown in Figure 4, given $\mathbf{a}^l \in \mathbb{R}^{B\times N\times C}$ with spatial size $B \times N \times C$ as the input from the l_{th} level of ViTs, the ASM first uses a sequential average pooling (SAP) to get sequential information for token-wise values. After that, to learn the per-token shift factor $\beta^l_{token} \in \mathbf{R}^{B\times N\times 1}$ for the original features, we adopt an efficient method that can be formulated as:

$$\beta^l_{token} = \mathbf{W}_2\, \sigma\left(\mathbf{W}_1\left(\frac{1}{C}\sum_{i=1}^{C}\mathbf{a}^l(i)\right)\right) \tag{11}$$

where σ represent ReLU, $\mathbf{W}_1 \in \mathbb{R}^{\frac{N}{r} \times N}$ and $\mathbf{W}_2 \in \mathbb{R}^{N \times \frac{N}{r}}$ denote the weights of two fully-connected (FC) layer. Similarly, we perform token-wise sequence pooling on $\mathbf{a}^l$ and learn channel-wise shift factors $\beta_n^l \in \mathbf{R}^{B \times 1 \times C}$ through two FC layers. In practice, we use 1×1 sequential convolution instead of FC layer to reduce the number of parameters and computation while preserving spatial information. Gernally, the procedure of ASM can be formulated as

$$\mathbf{a}_{asm}^l = (1 + \delta(\beta_{token}^l + \beta_{channel}^l)) \cdot \mathbf{a}^l \tag{12}$$

where δ denotes $\mathrm{Sigmoid}$ function that constrains the magnitude of the shift to be between 0 and 1. With the proposed ASM, the BinaryViT tunes the activation distribution before the sign function, which can mitigating the distortion caused by internal variation.

Differing from previous work, our ASM adopts a dynamic redistribution scheme on the activation of each layer, taking into consideration the variation of different inputs and learning token and channel wise shift factors accordingly, enabling the network to maintain more information during binarization.

5 Experiment

In this section, we construct extensive experiments on ImageNet [35] to demonstrate the effectiveness of the proposed BinaryViT. We first compare BinaryViT with previous state-of-the-art methods on different vision transformer structures. Moreover, we also perform ablation studies to verify the importance of each component in the proposed method.

5.1 Experiment settings

Dataset and models. We conduct all expreiments on ImageNet dataset [35], which contains over $1.2M$ training images and $50K$ validation images belonging to 1,000 classes and an 224×224 image size. The pre-processing and data augmentation follow the same protocols as in [12]. Specifically, we random sample 128 images from ImageNet training set as the mini-batch, and evaluate the BinaryViT using $1.5\times$ size of mini-batch on 4 NVIDIA A6000 GPUs with 48 GB memory. We adopt the Pytorch [29] and TIMM[2] library to implement the proposed BinaryViT on two popular vision transformer models: DeiT [39] and ViT [10]. The Top-1 accuracy of DeiT-Tiny, DeiT-Small, ViT-Small, and ViT-Base on ImageNet dataset are 72.1%, 79.8%, 81.4%, and 84.5% respectively.

Training configs. Before binarization, all parameters are initialized with the full-precision pretrained model. For all experiments, we employ the AdamW optimizer [47] with a weight decay set to 0. We set the initial learning rate to 1e-4, using a cosine annealing decay strategy and a 5-epoch warm up. The training of each stage count 100 epochs, and we set mini-lr to 1e-5 and 1e-6 for the first and second stage, respectively. Standard data augmentations [38] are applied with Default-style for DeiT and Inception-style for ViT, respectively. Additionally, we use hard knowledge distillation in all experiments, with λ_d set to 1. In particular, we use 8-bit instead of ± 1 for the first layer (patch embedding) and the last layer (classification head) following the common practice [22, 23, 25, 44].

5.2 Ablation Study

We begin by investigating the impact of various components. As demonstrated in Table 1, we establish DeiT-T [39] with vanilla binarization as the baseline and sequentially incorporate each of our contributions to better understand their individual effects on performance.

Initially, we introduce a learnable scaling factor for both weight and activation, yielding a 0.7% improvement. Next, we employ the two-stage training strategy, resulting in a 1.4% boost. Lastly, we apply logits KD to further enhance performance, which leads to a 2.0% improvement. In this end, we implement our strong baseline (row 5) as described in Section 3.

Compared to the strong baseline, our BinaryViT enhances performance by approximately 1.9%. Specifically, when GRS is applied, the distribution of latent weights is driven to bimodal (as shown in Figure 5), resulting in a 0.7% increase in Top-1 accuracy. Furthermore, ASM independently contributes to a 1.6% performance boost. These results emphasize that GRS and ASM individually enhance performance, and when combined, they significantly amplify the improvement, thus validating the effectiveness of the proposed GRS and ASM methods.

[2] https://github.com/rwightman/pytorch-image-models

Table 1: Ablation study of each component on ImageNet dataset [35] with DeiT-T[39]

	Method	$\text{Size}_{(\text{MB})}$	$\text{BOPs}_{(\text{M})}$	$\text{FLOPs}_{(\text{M})}$	$\text{OPs}_{(\text{M})}$	Top-1	Top-5
1	DeiT-T	22.9	0	1077.7	1077.7	72.1	91.1
2	Vanilla Binarization	1.0	1045.8	0.03	16.4	43.4	69.3
3	+ Learnable scaling factors	1.1	1045.8	0.03	16.4	44.1	69.6
4	+ Two-stage training	1.1	1045.8	0.03	16.4	45.5	71.1
5	+ logits KD (Strong Baseline)	1.1	1045.8	0.03	16.4	47.5	71.9
6	+ GRS	1.1	1045.8	0.03	16.4	48.2	72.7
7	+ ASM	1.5	1045.8	0.1	16.5	49.1	73.4
8	BinaryViT (ours)	1.5	1045.8	0.1	16.5	**49.4**	**73.6**

5.3 Main Results

We present experimental results on the ImageNet dataset [35] with various vision transformers in Table 2. In addition to comparing accuracy, we also examine the size and operations of the models.

Table 2: Comparison of the binarization results on ImageNet dataset[35]. '#Bits' (W-A) represents the bit widths for weight, activation in models. We also quantize the first and last layers to 8bit.

Model	Method	#Bits	$\text{Size}_{(\text{MB})}$	$\text{BOPs}_{(\text{G})}$	$\text{FLOPs}_{(\text{G})}$	$\text{OPs}_{(\text{G})}$	Top-1	Top-5
DeiT-T	Full-precision	32-32	22.87	0	1.07	1.07	72.11	91.14
	Baseline	1-1	1.07	1.05	0^*	0.02	47.52	71.93
	BinaryViT		1.51	1.05	0^*	0.02	**49.41**	**73.59**
DeiT-S	Full-precision	32-32	88.20	0	4.25	4.25	79.83	94.94
	Baseline	1-1	3.43	4.18	0.15	0.22	63.49	84.73
	BinaryViT		5.46	4.18	0.17	0.24	**65.54**	**86.03**
ViT-S	Full-precision	32-32	88.20	0	4.25	4.25	81.39	96.14
	Baseline	1-1	3.43	4.18	0.15	0.22	62.06	84.31
	BinaryViT		5.46	4.18	0.17	0.24	**63.75**	**85.38**
ViT-B	Full-precision	32-32	346.27	0	16.86	16.86	84.54	97.30
	Baseline	1-1	12.37	16.73	0.29	0.55	69.24	89.21
	BinaryViT		18.91	16.73	0.33	0.59	**71.91**	**90.64**

0^* represents 0.03M FLOPs, which can be considered negligible when measured in gigabytes (G).

For the DeiT-T backbone, our BinaryViT achieves a extreme compression ratio compared to the full-precision model. Notably, the proposed method significantly compresses the model size and OPs of DeiT-T by 15.1× and 53.5×. The proposed method improves the performance of the strong baseline by 1.9% with the same architecture, which is notable on the ImageNet dataset. With the addition of attention head and embedding dimension, the binary DeiT-S achieves 65.54%, surpassing the baseline by 2.05%. Our method substantially compresses the DeiT-S by 16.2× and 17.7× in model size and FLOPs, respectively.

Furthermore, our method produces convincing results on ViT. As shown in Table 2, the performance of the proposed method with ViT-S and ViT-B outperforms the baseline method by 1.69% and 2.67%, respectively, which is a significant margin. Compared to the full-precision model, our method attains a considerably higher compression rate and comparable performance. It is worth noting that our method compresses the model size and OPs of ViT-B by 18.3× and 28.6×, respectively. The results above underscore the significance of our BinaryViT.

5.4 Efficiency Analysis

Since the majority of parameters in BinaryViT are binary and require only 1 bit of memory in hardware, it is necessary to recalculate the size and operations of the model. Memory usage is

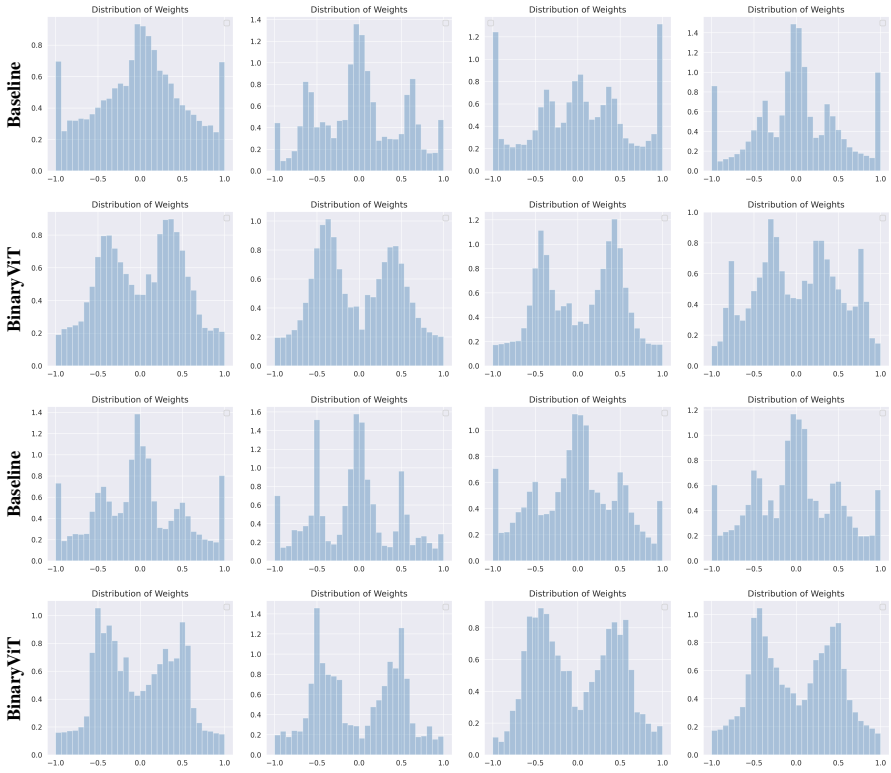

Figure 5: Visualization for the latent weight of Baseline (row 1, row 3) and BinaryViT (row2, row4). BinaryViT shows a bimodel distirbution, while baseline are heavily concentrated around 0 that increases the instability of the update step.

computed as the sum of 32 bits multiplied by the number of real-valued parameters and 1 bit multiplied by the number of binary parameters in the network. Given that the current generation of CPUs can perform bitwise XNOR operations and bit-counting in parallel with a 64-bit capacity, OPs are calculated as the sum of real-valued floating-point multiplications and 1/64 of the amount of 1-bit multiplications. Following [23, 25], we compute the total operations (OPs) as:

$$\text{OPs} = \frac{\text{BOPs}}{64} + \text{FLOPs} \tag{13}$$

When considering inference, the ASM with one sequential pooling layer and two 1×1 convolutions primarily consume FLOPs computational resources. Note that our ASM introduces a negligible floating-point computation overhead, as demonstrated in Table 1 and Table 2.

6 Conclusion

In this work, we have proposed an accurate full binarization scheme for ViTs, dubbed BinaryViT, to push the limit of the extreme quantization. We first established a strong baseline for binary ViTs by leveraging common techniques and identifying the sources of performance degradation, including weight oscillation and information distortion in activation. To mitigate these issues, we proposed a gradient regularization scheme to tackle weight oscillation and an activation shift module to tune the distribution of activation before binarization. Extensive experiments on the ImageNet dataset across various transformer architectures, such as DeiT and ViT, demonstrate the effectiveness of our BinaryViT. Specifically, our method achieves impressive savings of 16.2$\times$ and 17.7$\times$ in model size and OPs compared to the full-precision DeiT-S, while maintaining a competitive Top-1 accuracy of 65.54%. Our contributions provide a promising path to compress ViTs and improve their inference efficiency for real-world applications.

References

[1] Haoli Bai, Wei Zhang, Lu Hou, Lifeng Shang, Jin Jin, Xin Jiang, Qun Liu, Michael R. Lyu, and Irwin King. Binarybert: Pushing the limit of BERT quantization. In *Proc. of ACL/IJCNLP*, pages 4334–4348, 2021.

[2] Yoshua Bengio, Nicholas Léonard, and Aaron C. Courville. Estimating or propagating gradients through stochastic neurons for conditional computation. *arXiv preprint arXiv:1308.3432*, 2013.

[3] Daniel Bolya, Cheng-Yang Fu, Xiaoliang Dai, Peizhao Zhang, Christoph Feichtenhofer, and Judy Hoffman. Token merging: Your vit but faster. *arXiv preprint arXiv:2210.09461*, 2022.

[4] Daniel Bolya, Cheng-Yang Fu, Xiaoliang Dai, Peizhao Zhang, and Judy Hoffman. Hydra attention: Efficient attention with many heads. In *Proc. of ECCV Workshops*, pages 35–49, 2022.

[5] Adrian Bulat and Georgios Tzimiropoulos. Xnor-net++: Improved binary neural networks. In *Proc. of BMVC*, pages 1–12, 2019.

[6] Nicolas Carion, Francisco Massa, Gabriel Synnaeve, Nicolas Usunier, Alexander Kirillov, and Sergey Zagoruyko. End-to-end object detection with transformers. In *Proc. of ECCV*, pages 213–229, 2020.

[7] Chun-Fu (Richard) Chen, Quanfu Fan, and Rameswar Panda. Crossvit: Cross-attention multi-scale vision transformer for image classification. In *Proc. of ICCV*, pages 347–356, 2021.

[8] Matthieu Courbariaux, Yoshua Bengio, and Jean-Pierre David. Binaryconnect: Training deep neural networks with binary weights during propagations. In *Proc. of NeurIPS*, pages 3123–3131, 2015.

[9] Tri Dao, Daniel Y. Fu, Stefano Ermon, Atri Rudra, and Christopher Ré. Flashattention: Fast and memory-efficient exact attention with io-awareness. In *Proc. of NeurIPS*, 2022.

[10] Alexey Dosovitskiy, Lucas Beyer, Alexander Kolesnikov, Dirk Weissenborn, Xiaohua Zhai, Thomas Unterthiner, Mostafa Dehghani, Matthias Minderer, Georg Heigold, Sylvain Gelly, et al. An image is worth 16x16 words: Transformers for image recognition at scale. *arXiv preprint arXiv:2010.11929*, 2020.

[11] Steven K. Esser, Jeffrey L. McKinstry, Deepika Bablani, Rathinakumar Appuswamy, and Dharmendra S. Modha. Learned step size quantization. In *Proc. of ICLR*, 2020.

[12] Kaiming He, Xiangyu Zhang, Shaoqing Ren, and Jian Sun. Deep residual learning for image recognition. In *Proc. of CVPR*, pages 770–778, 2016.

[13] Yang He, Guoliang Kang, Xuanyi Dong, Yanwei Fu, and Yi Yang. Soft filter pruning for accelerating deep convolutional neural networks. In *Proc. of IJCAI*, pages 2234–2240, 2018.

[14] Jack Lanchantin, Tianlu Wang, Vicente Ordonez, and Yanjun Qi. General multi-label image classification with transformers. In *Proc. of CVPR*, pages 16478–16488, 2021.

[15] Yanjing Li, Sheng Xu, Baochang Zhang, Xianbin Cao, Peng Gao, and Guodong Guo. Q-vit: Accurate and fully quantized low-bit vision transformer. In *Proc. of NeurIPS*, 2022.

[16] Zhikai Li, Liping Ma, Mengjuan Chen, Junrui Xiao, and Qingyi Gu. Patch similarity aware data-free quantization for vision transformers. In *Proc. of ECCV*, pages 154–170, 2022.

[17] Zhikai Li, Junrui Xiao, Lianwei Yang, and Qingyi Gu. Repq-vit: Scale reparameterization for post-training quantization of vision transformers. *arXiv preprint arXiv:2212.08254*, 2022.

[18] Sihao Lin, Hongwei Xie, Bing Wang, Kaicheng Yu, Xiaojun Chang, Xiaodan Liang, and Gang Wang. Knowledge distillation via the target-aware transformer. In *Proc. of CVPR*, pages 10905–10914, 2022.

[19] Yang Lin, Tianyu Zhang, Peiqin Sun, Zheng Li, and Shuchang Zhou. Fq-vit: Fully quantized vision transformer without retraining. *arXiv preprint arXiv:2111.13824*, 2021.

[20] Yuhan Lin, Lingfeng Niu, Yang Xiao, and Ruizhi Zhou. Diluted binary neural network. *Pattern Recognition*, 2023.

[21] Ze Liu, Yutong Lin, Yue Cao, Han Hu, Yixuan Wei, Zheng Zhang, Stephen Lin, and Baining Guo. Swin transformer: Hierarchical vision transformer using shifted windows. In *Proc. of ICCV*, pages 10012–10022, 2021.

[22] Zechun Liu, Barlas Oguz, Aasish Pappu, Lin Xiao, Scott Yih, Meng Li, Raghuraman Krishnamoorthi, and Yashar Mehdad. Bit: Robustly binarized multi-distilled transformer. In *Proc. of NeurIPS*, 2022.

[23] Zechun Liu, Zhiqiang Shen, Marios Savvides, and Kwang-Ting Cheng. Reactnet: Towards precise binary neural network with generalized activation functions. In *Proc. of ECCV*, pages 143–159, 2020.

[24] Zhenhua Liu, Yunhe Wang, Kai Han, Wei Zhang, Siwei Ma, and Wen Gao. Post-training quantization for vision transformer. In *Proc. of NeurIPS*, pages 28092–28103, 2021.

[25] Brais Martínez, Jing Yang, Adrian Bulat, and Georgios Tzimiropoulos. Training binary neural networks with real-to-binary convolutions. In *Proc. of ICLR*, 2020.

[26] Sachin Mehta and Mohammad Rastegari. Mobilevit: Light-weight, general-purpose, and mobile-friendly vision transformer. In *Proc. of ICLR*, 2022.

[27] Lingchen Meng, Hengduo Li, Bor-Chun Chen, Shiyi Lan, Zuxuan Wu, Yu-Gang Jiang, and Ser-Nam Lim. Adavit: Adaptive vision transformers for efficient image recognition. In *Proc. of CVPR*, pages 12299–12308, 2022.

[28] Eriko Nurvitadhi, David Sheffield, Jaewoong Sim, Asit K. Mishra, Ganesh Venkatesh, and Debbie Marr. Accelerating binarized neural networks: Comparison of fpga, cpu, gpu, and asic. In *Proc. of FPT*, pages 77–84, 2016.

[29] Adam Paszke, Sam Gross, Francisco Massa, Adam Lerer, James Bradbury, Gregory Chanan, Trevor Killeen, Zeming Lin, Natalia Gimelshein, Luca Antiga, Alban Desmaison, Andreas Köpf, Edward Yang, Zach DeVito, Martin Raison, Alykhan Tejani, Sasank Chilamkurthy, Benoit Steiner, Lu Fang, Junjie Bai, and Soumith Chintala. Pytorch: An imperative style, high-performance deep learning library. *arXiv*, abs/1912.01703, 2019.

[30] Haotong Qin, Yifu Ding, Mingyuan Zhang, Qinghua Yan, Aishan Liu, Qingqing Dang, Ziwei Liu, and Xianglong Liu. Bibert: Accurate fully binarized BERT. In *Proc. of ICLR*, 2022.

[31] Haotong Qin, Ruihao Gong, Xianglong Liu, Mingzhu Shen, Ziran Wei, Fengwei Yu, and Jingkuan Song. Forward and backward information retention for accurate binary neural networks. In *Proc. of CVPR*, pages 2247–2256, 2020.

[32] Yongming Rao, Wenliang Zhao, Benlin Liu, Jiwen Lu, Jie Zhou, and Cho-Jui Hsieh. Dynamicvit: Efficient vision transformers with dynamic token sparsification. In *Proc. of NeurIPS*, pages 1–14, 2021.

[33] Mohammad Rastegari, Vicente Ordonez, Joseph Redmon, and Ali Farhadi. Xnor-net: Imagenet classification using binary convolutional neural networks. In *Proc. of ECCV*, pages 525–542, 2016.

[34] Adriana Romero, Nicolas Ballas, Samira Ebrahimi Kahou, Antoine Chassang, Carlo Gatta, and Yoshua Bengio. Fitnets: Hints for thin deep nets. In *Proc. of ICLR*, pages 1–13, 2015.

[35] Olga Russakovsky, Jia Deng, Hao Su, Jonathan Krause, Sanjeev Satheesh, Sean Ma, Zhiheng Huang, Andrej Karpathy, Aditya Khosla, Michael Bernstein, Alexander C. Berg, and Li Fei-Fei. Imagenet large scale visual recognition challenge. *International Journal of Computer Vision*, 115(3):211–252, 2015.

[36] Mark Sandler, Andrew G. Howard, Menglong Zhu, Andrey Zhmoginov, and Liang-Chieh Chen. Mobilenetv2: Inverted residuals and linear bottlenecks. In *Proc. of CVPR*, pages 4510–4520, 2018.

[37] Robin Strudel, Ricardo Garcia Pinel, Ivan Laptev, and Cordelia Schmid. Segmenter: Transformer for semantic segmentation. In *Proc. of ICCV*, pages 7242–7252, 2021.

[38] Christian Szegedy, Vincent Vanhoucke, Sergey Ioffe, Jonathon Shlens, and Zbigniew Wojna. Rethinking the inception architecture for computer vision. pages 2818–2826, 2015.

[39] Hugo Touvron, Matthieu Cord, Matthijs Douze, Francisco Massa, Alexandre Sablayrolles, and Hervé Jégou. Training data-efficient image transformers & distillation through attention. In *Proc. of ICML*, pages 10347–10357, 2021.

[40] Wenhai Wang, Enze Xie, Xiang Li, Deng-Ping Fan, Kaitao Song, Ding Liang, Tong Lu, Ping Luo, and Ling Shao. Pyramid vision transformer: A versatile backbone for dense prediction without convolutions. In *Proc. of ICCV*, pages 568–578, 2021.

[41] Junrui Xiao, He Jiang, Zhikai Li, and Qingyi Gu. Rethinking prediction alignment in one-stage object detection. *Neurocomputing*, 514:58–69, 2022.

[42] Junrui Xiao, He Jiang, Zhikai Li, and Qingyi Gu. Dcifpn: Deformable cross-scale interaction feature pyramid network for object detection. *IET Image Processing*, 2023.

[43] Junrui Xiao, Zhikai Li, Lianwei Yang, and Qingyi Gu. Patch-wise mixed-precision quantization of vision transformer. 2023.

[44] Sheng Xu, Yanjing Li, Teli Ma, Mingbao Lin, Hao Dong, Baochang Zhang, Peng Gao, and Jinhu Lv. Resilient binary neural network. 2023.

[45] Sheng Xu, Yanjing Li, Bohan Zeng, Teli Ma, Baochang Zhang, Xianbin Cao, Peng Gao, and Jinhu Lu. Ida-det: An information discrepancy-aware distillation for 1-bit detectors. *arXiv preprint arXiv:2210.03477*, 2022.

[46] Yifan Xu, Zhijie Zhang, Mengdan Zhang, Kekai Sheng, Ke Li, Weiming Dong, Liqing Zhang, Changsheng Xu, and Xing Sun. Evo-vit: Slow-fast token evolution for dynamic vision transformer. In *Proc. of AAAI*, pages 2964–2972, 2022.

[47] Yang You, Jing Li, Sashank Reddi, Jonathan Hseu, Sanjiv Kumar, Srinadh Bhojanapalli, Xiaodan Song, James Demmel, Kurt Keutzer, and Cho-Jui Hsieh. Large batch optimization for deep learning: Training bert in 76 minutes. In *Proc. of ICLR*, pages 1–37, 2020.

[48] Fang Yu, Kun Huang, Meng Wang, Yuan Cheng, Wei Chu, and Li Cui. Width & depth pruning for vision transformers. In *Proc. of AAAI*, pages 3143–3151, 2022.

[49] Zhihang Yuan, Chenhao Xue, Yi-Qiang Chen, Qiang Wu, and Guangyu Sun. Ptq4vit: Post-training quantization for vision transformers with twin uniform quantization. In *Proc. of ECCV*, 2022.

[50] Sixiao Zheng, Jiachen Lu, Hengshuang Zhao, Xiatian Zhu, Zekun Luo, Yabiao Wang, Yanwei Fu, Jianfeng Feng, Tao Xiang, Philip H. S. Torr, and Li Zhang. Rethinking semantic segmentation from a sequence-to-sequence perspective with transformers. In *Proc. of CVPR*, pages 6881–6890, 2021.